Distribution and bioactivity of the Ret-specific D4 aptamer in three-dimensional collagen gel cultures

Maria Teresa Vento,[1] Marco Iuorio,[1] Paolo A. Netti,[1,3] Frederic Ducongè,[4] Bertrand Tavitian,[4] Vittoriode Franciscis,[2] and Laura Cerchia[2]

[1]Interdisciplinary Research Centre on Biomedical Materials and Department of Materials and Production Engineering, University of Naples Federico II; [2]Istituto di Endocrinologia ed Oncologia Sperimentale del CNR ''G. Salvatore,'' Naples, Italy; [3]Istituto Italiano di Tecnologia, Genoa, Italy; and [4]CEA/DSV/DRM Service Hospitalier Frederic Joliot, INSERM E-103, Orsay, France

Abstract

The success of tyrosine kinase inhibitors in cancer therapy prompted intensive research efforts addressed to the development of new specific diagnostics and therapeutics. Targeting large transmembrane molecules, including receptor tyrosine kinases, is a major pharmacologic challenge. The D4 RNA-aptamer, isolated applying the Systematic Evolution of Ligand by Exponential Enrichment procedure on living cells, has been proven a specific inhibitor of the human receptor tyrosine kinase Ret. In our attempts to generate new powerful probes for *in vivo* applications, in the present study, we addressed the ability of D4 to preserve its biological activity in cells embedded in three-dimensional collagen gels. These matrices provide a microenvironment mimicking the cell organization as seen *in vivo*, thus representing a suitable tool to approach the use of the aptamer *in vivo*. By taking advantage of transformed fibroblasts expressing Ret as a model system, we showed that the cells maintain normal phenotype and growth patterns when cultured in three-dimensional matrices and that the D4 aptamer preserves its ability to inhibit Ret on the surface of the cells embedded in collagen. Because the biological activity of RNA aptamers is largely dictated by their folded structure, the results indicate that a folded conformation of D4 responsible of its inhibiting function is preserved in the three-dimensional constructs, thus supporting its use in tumors *in vivo*. [Mol Cancer Ther 2008;7(10):3381–8]

Received 5/2/08; revised 7/25/08; accepted 7/27/08.

Grant support: CNR, European Molecular Imaging Laboratory Network grant LSH-2004-503569, MIUR-FIRB grant RBIN04J4J7, and Associazione Italiana per la Ricerca sul Cancro (L. Cerchia).

The costs of publication of this article were defrayed in part by the payment of page charges. This article must therefore be hereby marked *advertisement* in accordance with 18 U.S.C. Section 1734 solely to indicate this fact.

Requests for reprints: Laura Cerchia, Istituto di Endocrinologia ed Oncologia Sperimentale del CNR ''G. Salvatore,'' via S. Pansini 5, 80131 Naples, Italy. Phone: 39-817462036; Fax: 39-817701016. E-mail: cerchia@unina.it

doi:10.1158/1535-7163.MCT-08-0580

Introduction

The proto-oncogene Ret (rearranged during transfection) encodes a receptor protein-tyrosine kinase, which is highly expressed in the developing central and peripheral nervous system and in excretory system. Gain-of-function mutations in the Ret gene cause inherited predisposition to cancer in multiple endocrine neoplasia types 2A (MEN2A) and 2B (MEN2B). Both classes of mutations lead to constitutive activation of Ret intrinsic tyrosine kinase activity (1, 2).

Recently, we adopted a whole-cell Systematic Evolution of Ligand by Exponential Enrichment strategy to obtain nuclease-resistant RNA-based aptamers that, because of their folded structure, recognize the human Ret on the cell surface. One of these aptamers, named D4, binds to Ret at high affinity, displaying a K_d value of 30 nmol/L, blocking receptor activity and its dependent intracellular signaling pathways (3–5).

However, whether nucleic acid aptamers may preserve their folded structure, and then their biological function, when crossing biological barriers is still largely unknown. Thus, the understanding of the biophysical properties of aptamers in a three-dimensional biological environment becomes critical to their development as therapeutic or diagnostic tools. Because, *in vivo*, cells exist in extracellular matrix environment rich in type I collagen, cells cultured in three-dimensional matrices better reflect *in vivo* cell physiology when compared with traditional two-dimensional systems (6–8). Therefore, three-dimensional culture systems that simulate the collagen-rich extracellular matrix of normal and tumoral tissue may be appropriate to test cancer cell potential for invasion and for tumor cell sensitivity to anticancer drugs.

In this article, we have evaluated the stability, the diffusion, and the targeting function of the Ret antagonist aptamer by taking advantage of an *in vitro* system consisting of three-dimensional cultures of cells immobilized in collagen matrices. Our results show that the D4 aptamer fully retains its biological properties (binding to Ret receptor and inhibition of its tyrosine kinase activity) within physiologically relevant *in vivo*-like, cell-derived three-dimensional matrices.

Materials and Methods

Generation of Labeled D4 Aptamer

D4 is a 93-bp RNA aptamer containing 2′-fluoropyrimidine modifications that specifically binds to the extracellular region of Ret receptor either wild-type (Ret^{wt}) or mutated (Ret^{C634Y}), thus inhibiting its ligand-induced or constitutive tyrosine kinase activity, respectively (3).

D4Sc is the scrambled inactive control aptamer. D4 and D4Sc have been labeled with the rhodamine (Alexa Fluor 532) probe according to the Ulysis Nucleic Acid Labeling Kit (Molecular Probes/Invitrogen) instructions. The method is

based on the use of a platinum-fluorophore complex that forms a stable adduct with N7 position of guanine and, to a lesser extent, adenine bases in oligonucleotides. Following the labeling reaction, the separation of RNA from the unreacted reagent has been accomplished through the use of a spin-column procedure (Micro Bio-Spin P30; Bio-Rad). Hereafter, we indicate the rhodamine-labeled D4 and D4Sc aptamers as $D4^{Alexa}$ and $D4Sc^{Alexa}$, respectively.

Classical Two-Dimensional Cell Culture, Immunoblotting Analysis, and Aptamer Treatments

Growth conditions, in classic two-dimensional cultures, for NIH3T3, NIH/MEN2A (NIH3T3 cells stably transfected with vector-expressing human Ret^{C634Y} mutant receptor), and PC12/MEN2A (PC12 cells stably transfected with vector-expressing human Ret^{C634Y}) cells were described previously (3).

Binding experiments of radiolabeled aptamers (or the scrambled sequences as controls) to PC12/MEN2A were done in 24-well plates in triplicate with 5′-^{32}P-labeled RNA as reported previously (3).

To verify the inhibiting effect on Ret activity of D4 aptamer after the labeling reaction, the fluorescent aptamer was subjected to a short denaturation-renaturation step and then incubated for 1 h at the indicated amount on NIH/MEN2A cells (160,000 per 3.5 cm plate) previously serum starved for 2 h. Preparation of cell extracts and immunoblotting analysis were done as described (9). The primary antibodies used were the following: anti-Ret (H-300) and anti-extracellular signal-regulated kinase (ERK) 1 (C-16; Santa Cruz Biotechnology) and anti-(Tyr^{905}-phosphorylated) Ret (pRet), anti-phospho-p44/42 mitogen-activated protein kinase (pERK), and anti-cyclin D1 (Cell Signaling).

To evaluate the distribution of D4 on NIH/MEN2A cells surface, 30,000 cells grown on a sterile glass coverslip in a tissue culture dish were left untreated or treated with 500 nmol/L $D4^{Alexa}$ or $D4Sc^{Alexa}$; following 10 min incubation at 37°C, cells were washed three times in cold PBS and fixed in 4% paraformaldehyde in PBS for 10 min on ice. The coverslips were washed with PBS and mounted on slides in 1:1 glycerol/PBS and the cells were visualized by confocal microscopy.

Immunofluorescence Analysis

Fixed NIH/MEN2A cells following $D4^{Alexa}$ treatment grown on glass coverslips were washed three times in PBS and fixed in 4% paraformaldehyde in PBS for 10 min at room temperature. Paraformaldehyde was quenched with 10 mmol/L ammonium chloride, and cells were permeabilized with PBS, 0.1% Triton X-100 for 5 min at room temperature. The coverslips were washed three times in PBS and then blocked in PBS, 0.5% bovine serum albumin for 30 min. Cells were incubated with anti-pRet (Tyr^{1062}; Santa Cruz Biotechnology) primary antibody diluted in PBS, 0.5% bovine serum albumin for 1 h at room temperature. Coverslips were washed five times in PBS and treated for 1 h at room temperature with goat anti-rabbit secondary antibodies coupled to fluorescein (Invitrogen) diluted in PBS, 0.5% bovine serum albumin. Coverslips were washed and mounted and the cells were visualized by confocal microscopy.

Preparation of Collagen Gels and Fluorescence Correlation Spectroscopy Analysis

Vitrogen 100 collagen type I was purchased from Collagen (Cohesion Technologies). The pH and ionic strength were adjusted by addition of NaOH (pH 7.4) and 10× culture medium. To obtain a collagen gel formed predominantly of fibers, the neutralized collagen type I was polymerized at 37°C for 1 h.

The fluorescence correlation spectroscopy (FCS) measurements (10) were carried out by using a confocal microscope, LSM510 Confocor2, equipped with the FCS module (Carl Zeiss).

The fluorescence of rhodamine-labeled aptamer was excited by argon laser (λ = 514 nm) and the emission was collected within the range λ = 530 to 600 nm. FCS measurements were conducted in eight-well chamber slides with borosilicate coverslip (Lab-Tek Chamber Slide; Nalge Nunc International) at ~20°C by using a total volume of 250 μL. Dilutions were done in PBS or water. All measure-

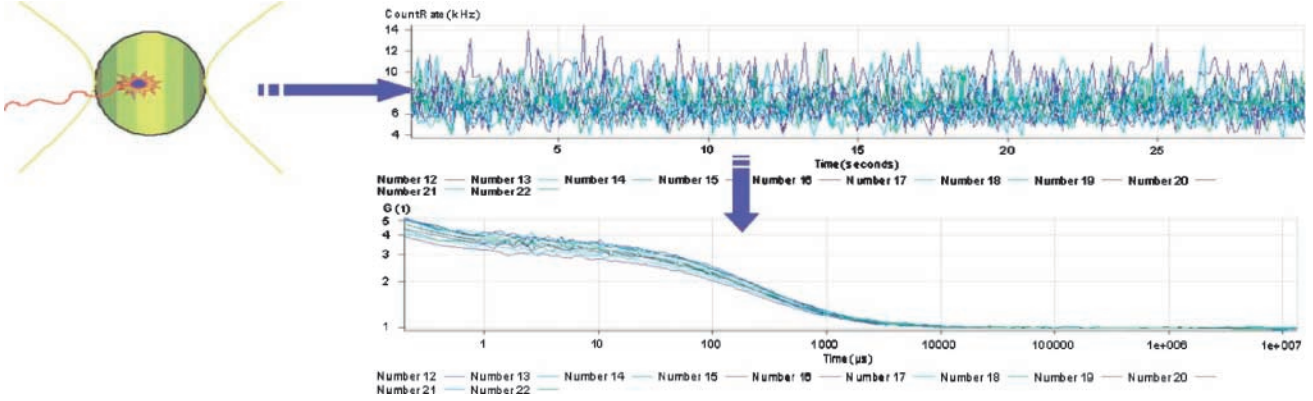

Figure 1. Schematic representation of principles of FCS measurements. The illuminated confocal volume is approximately of 1 fl and the fluorescence light due to the photon bursts of the few fluorescing molecules present within the volume is monitored by a high-sensitivity photon counter. The fluorescence intensity fluctuation deriving from molecular trafficking within the confocal volume is registered and correlated.

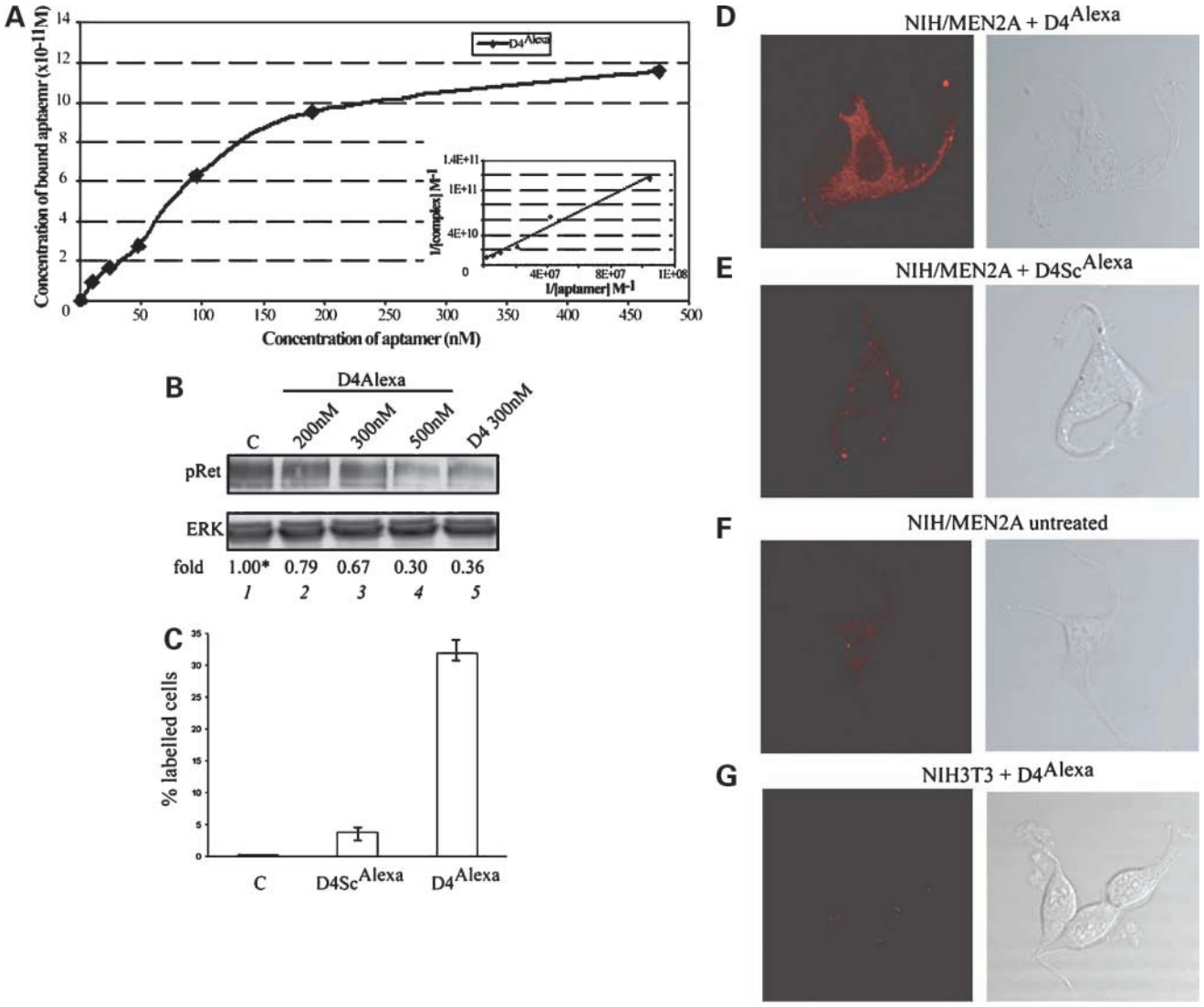

Figure 2. Fluorescent D4 specifically binds to Ret mutant-expressing cells in two-dimensional cultures. **A,** binding curve of the $D4^{Alexa}$ aptamer on PC12/MEN2A. $D4^{Alexa}$ was 5′-^{32}P-radiolabeled and incubated at different concentrations on cell monolayers. The background binding value for a fluorescent D4 scrambled sequence ($D4Sc^{Alexa}$) is subtracted from every data point. Lineweaver Burk analysis (*inset*) was used for the evaluation of the binding constant. **B,** NIH/MEN2A cells were treated with increasing concentration of $D4^{Alexa}$ (*lanes 2-4*) or with 300 nmol/L unlabeled D4 (*lane 5*). **C,** mock-treated cells (*lane 1*). Cell lysates were immunoblotted with anti-pRet antibodies. Equal loading was confirmed by immunoblotting with anti-ERK antibodies. Quantitations are done on the sum of the two Ret-specific enhanced chemiluminescence bands of 170 and 150 kDa corresponding to different glycosylation states of Ret. Intensity of bands have been calculated using the NIH Image Program on at least two different expositions to assure the linearity of each acquisition. Fold values are expressed relative to the reference points, arbitrarily set to 1 (*asterisk*). Representative of at least three independent experiments. **C** to **G,** following the treatment with the indicated labeled aptamer, NIH/MEN2A (**D-F**) or NIH3T3 (**G**) were visualized by confocal microscopy and photographed. The percentage of cells labeled with $D4^{Alexa}$ or $D4Sc^{Alexa}$ was calculated and reported as histogram (**C**). *Columns,* average of three independent experiments.

ments were done with a ×40 water objective(C-Apochromat 40×/1,2W Korr, numerical aperture 1.2; Carl Zeiss).

Before each series of measurements, the signal-to-noise ratio was optimized by maximizing the photon count rate per molecules, which was typically about 40. To optimize the signal acquisition, the time of each measurement was set at 10 s plus 3 s of prebleach. For each specimen, the characteristic diffusion time and the number of particles in the confocal volume were evaluated as an average over at least 20 measurements for each specimen. The confocal volume was determined by calibrating the optical volume with a solution of 10^{-7} mol/L rhodamine6G. Because the diffusion coefficient of the rhodamine6G is known (D = 2.72e-6 cm^2/s), ω_1 can be estimated by the formula: $D = (\omega_1)^2/4\tau_D$, and used for the evaluation of the diffusion coefficient of any other molecule: the confocal volume resulted of 1.6 fl.

The schematic principles of FCS measurements are illustrated in the Fig. 1. The analysis is realized by correlating the fluctuation signals over a statistical

significant number of samples by the autocorrelation function and fitting the curve obtained with the following function:

$$G_{\text{total}}(\tau)\cdot = \frac{1}{N}\cdot\left[\frac{1}{(1+\frac{\tau}{\tau_D})}\cdot\frac{1}{\sqrt{1+(\frac{r_0}{z_0})^2\cdot\frac{\tau}{\tau_D}}}\right]+1$$

to obtain the characteristic diffusion time (τ_D) and the average number of molecules in the control volume, where N is the average number of molecules within the confocal volume approximated as a three-dimensional Gaussian, which is decayed to $1/e^2$ at r_0 in lateral direction and at z_0 in the axial direction. From the diffusion characteristic time (τ_D), the diffusion coefficient (D) results as:

$$D = \frac{\omega_1^2}{4\tau_D}$$

Generation of Three-Dimensional Cell Constructs and Aptamer Treatments

NIH3T3 or NIH/MEN2A (65,000 cells) were suspended in 200 μL neutralized collagen solution to obtain a final concentration of 1.2 mg/mL. Cells embedded in collagen gel were grown in chamber slides with borosilicate coverslip. After collagen gel polymerization, phase-contrast light microscopy revealed that the cells were uniformly dispersed within gel (2 mm thin). The cells were cultured in the same complete medium as in two-dimensional cultures for the time of the experiments.

To evaluate the inhibiting effect of D4 on NIH/MEN2A in three-dimensional matrices, cells were washed with prewarmed DMEM before the addition of the aptamer and then incubated at 37°C with 3.25 μmol/L aptamer previously subjected to a short denaturation-renaturation step. The concentration of the aptamer was calculated to ensure the continuous presence of at least 200 nmol/L taking into account the half-life of D4 aptamer in 10% serum (~6 h). Following 20 h treatment, cells were removed from the three-dimensional collagen by using a solution of 2.5 mg/mL collagenase I (Sigma) in PBS prewarmed at 37°C. One gel volume of the prewarmed collagenase solution was added to completely submerge the portion of the gel to be digested and then incubated at 37°C for 15 min by gently pipetting the collagenase/gel solution up and down to facilitate the degradation of the gel. Cells were spinned out, the cellular pellet was processed for the whole protein extract, and immunoblot-

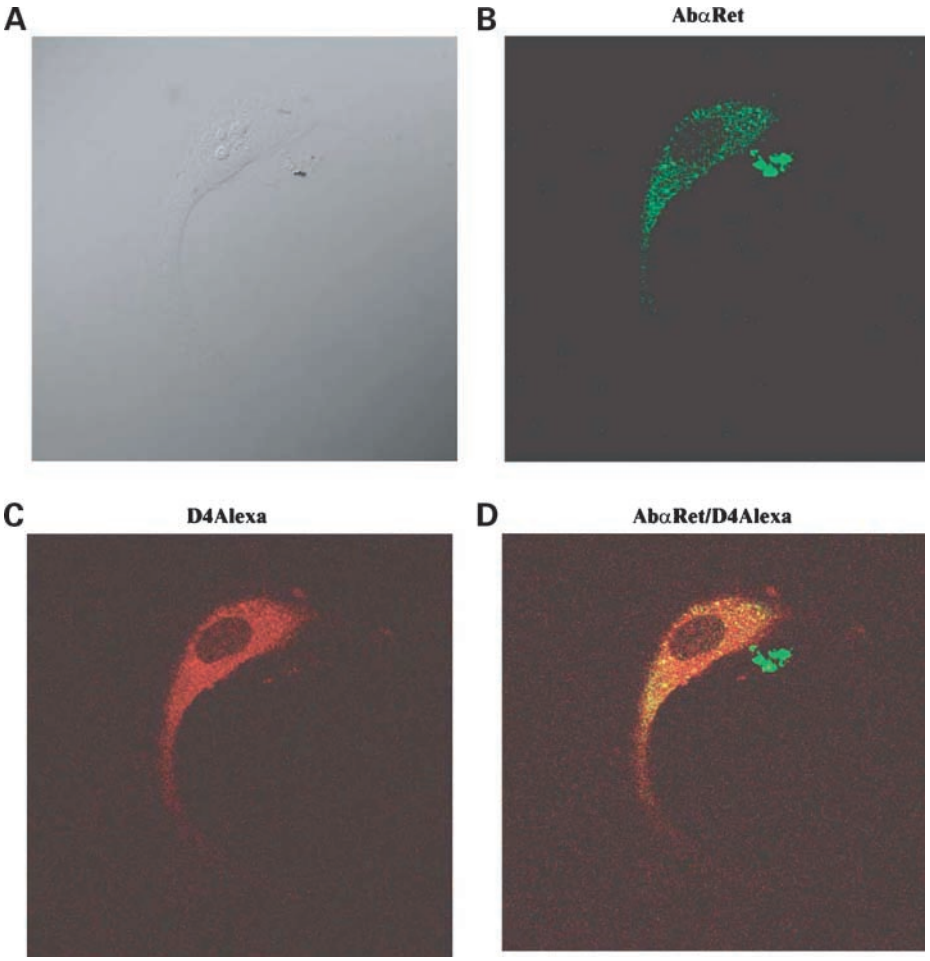

Figure 3. D4 aptamer and Ret-specific antibody colocalize on NIH/MEN2A. **A,** NIH/MEN2A cells were visualized by confocal microscopy and photographed. **B,** cells were stained with anti-pRet (Tyr^{1062}) primary antibodies followed by fluorescein-conjugated anti-rabbit antibodies (*green*). **C,** cells treated with $D4^{Alexa}$ (*red*). **D,** colocalization (*yellow*) of Ret antibodies and $D4^{Alexa}$. The excitation wavelengths were 488 nm for Alexa Fluor 532 rhodamine-labeled aptamer and for fluorescein-conjugated secondary antibodies. All digital images were captured at the same setting to allow direct comparison of staining patterns. Final images were processed using Adobe Photoshop software.

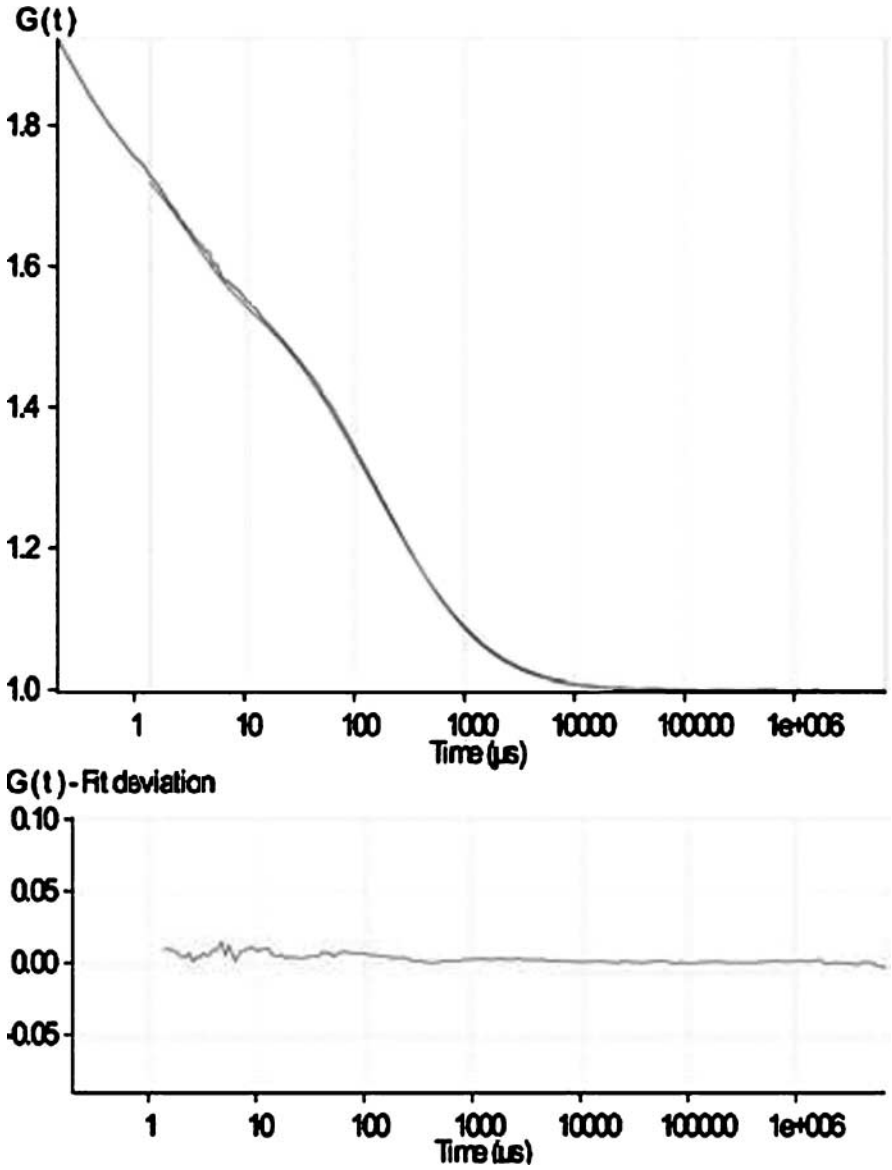

Figure 4. FCS to determine the diffusion of D4 aptamer in collagen gels. FCS fit to determine the presence of labeled aptamer in proximity of coverslip after time of 24 h.

ting analysis was done as reported above for two-dimensional classic cell culture.

To visualize D4 on cell surface, NIH/MEN2A cells were treated with 5 μmol/L $D4^{Alexa}$ or $D4Sc^{Alexa}$ (to ensure the continuous presence of an aptamer concentration of at least 600 nmol/L, taking into account of its half-life) at 37°C in the presence of 100 μg/mL tRNA as a nonspecific competitor used to saturate the collagen electrostatic charges. Following 20 h incubation, cells were processed as described.

Results and Discussion

Inhibiting Effect and Localization of Fluorescent D4 Aptamer on NIH/MEN2A Cells in Two-Dimensional Cultures

To visualize the D4 aptamer on surface of NIH/MEN2A cells in both two-dimensional and three-dimensional systems, the aptamer has been labeled by the attachment of fluorescent Alexa rhodamine probe. The used procedure allows to couple the fluorescent dye to purine bases in the RNA aptamers. First, we wondered whether the covalent attachment of the Alexa probe to D4 may affect its K_d of 30 nmol/L (3). To this aim, binding analyses with the fluorescent-labeled D4 (that we named $D4^{Alexa}$) was done on PC12/MEN2A cells (see Materials and Methods). As shown (Fig. 2A), the fluorescent dye coupling did not hamper the ability of the aptamer to bind the target cells even if with a higher K_d (100 nmol/L value). Next, we looked at the inhibiting effect of $D4^{Alexa}$ on Ret activity. Thus, NIH/MEN2A cells were either left untreated or treated for 1 h with increasing concentrations of $D4^{Alexa}$ or the unlabeled D4 aptamer. As shown in Fig. 2B, $D4^{Alexa}$ was effective in

inhibiting Ret^{C634Y} autophosphorylation up to 70% and its effect at 500 nmol/L is very close to the one of D4 at 300 nmol/L compatible with the reduced binding affinity of $D4^{Alexa}$ compared to D4.

Furthermore, NIH/MEN2A cells were left untreated or treated for 5 or 10 min at 37°C with increasing amount of $D4^{Alexa}$ or $D4Sc^{Alexa}$ and then visualized by confocal microscopy. A specific distribution of rhodamine-labeled D4 on cell surface occurred; following 10 min at 37°C, in the presence of 500 nmol/L aptamer concentration, the percentage of cells labeled with the $D4^{Alexa}$ was of 30% with respect to 3.7% obtained with $D4Sc^{Alexa}$ (Fig. 2C-F). No distribution of the $D4^{Alexa}$ aptamer on parental NIH3T3 cells was obtained (Fig. 2G).

To further characterize the identity of the binding of the fluorescent D4 aptamer to Ret-expressing cells, labeling with $D4^{Alexa}$ was combined with staining with a specific Ret antibody (Fig. 3). An extensive overlap of Ret antibody and $D4^{Alexa}$ respective fluorescent signals was observed in any of fields examined by confocal microscopy, thus indicating a clear colocalization of the aptamer and the antibody on the receptor expressed on cell surface.

Taken together, these results show that the labeling procedure used for the attachment of the rhodamine probe to the aptamer preserve its strong affinity for Ret, thus providing the first imaging of a fluorescent aptamer on cell surface.

Diffusion of D4 in Collagen Gels

FCS was used to determine the diffusion constant by monitoring the Brownian movement of individual fluorescent-tagged molecule in solution as well as in collagen gels. The decay times of tagged aptamer in solution could be well described with a single exponential function, indicating the monomodal size distribution of the fluorophores in solution. On the other hand, the fluctuation time series did not correlate with a single exponential decay when the tagged aptamers were diffusing in collagen gels and a double exponential function was necessary to fit the data (Fig. 4). By using FCS measurements, we determined a 24 h time for the fluorescent-labeled D4 to cross entirely the collagen gels. Indeed, when tagged aptamers reach a z-quote of 200 μm from the coverslip, they can be detected based on their characteristic decay time (Fig. 4).

Inhibiting Effect and Localization of Fluorescent D4 Aptamer on NIH/MEN2A Cells in Three-Dimensional Cultures

NIH/MEN2A transformed fibroblasts appear a highly suitable model system to evaluate the targeting properties of the D4 aptamer in three-dimensional cell cultures. Indeed, we have shown previously that, on expression of Ret^{C634Y} mutant receptor, NIH3T3 cells show drastic changes in their morphology and that D4 is able to specifically revert the transformed phenotype by inhibiting the constitutive signaling from Ret^{C634Y} in NIH/MEN2A cells cultured in classic two-dimensional cultures (3). Furthermore, as shown above (Figs. 2 and 3), a good distribution of the fluorescent $D4^{Alexa}$ on transformed fibroblasts surface indicates these cells as an appropriate tool to follow the D4 ability to hit the Ret receptor in three-dimensional NIH/MEN2A cultures.

Reconstituted bovine type I collagen gels form a stable matrix for cell suspension culture. When examined by

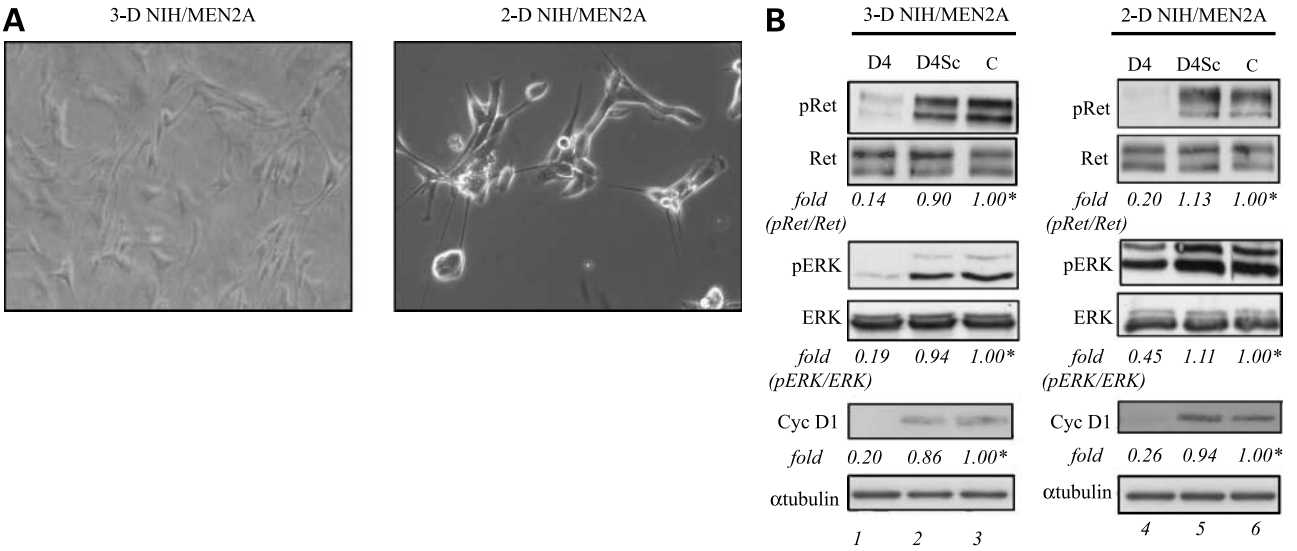

Figure 5. D4 specifically inhibits Ret activity in NIH/MEN2A cells cultured in three-dimensional cultures. **A,** NIH/MEN2A cells cultured in three-dimensional matrices (*left*) or two-dimensional cultures (*right*) were visualized by phase-contrast light microscopy and photographed. **B,** cells in three-dimensional (*left*) or two-dimensional (*right*) cultures were treated with D4 (*lanes 1* and *4*, respectively) or D4Sc (*lanes 2* and *5*, respectively); **C,** mock-treated cells (*lanes 1* and *6*). Cell lysates were immunoblotted with anti-pRet or anti-pERK antibodies as indicated. To confirm equal loading, the filters were stripped and reprobed with anti-Ret or anti-ERK antibodies, respectively. To follow the expression of cell cycle-related protein, cyclin D1, lysates were immunoblotted with anti-cyclin D1 antibodies and the filters were blotted with anti-α-tubulin antibodies to normalize the loaded proteins as indicated. Quantitation and relative abundances are expressed relative to controls, arbitrarily set to 1 (*asterisk*; see Fig. 2B). Representative of at least three independent experiments.

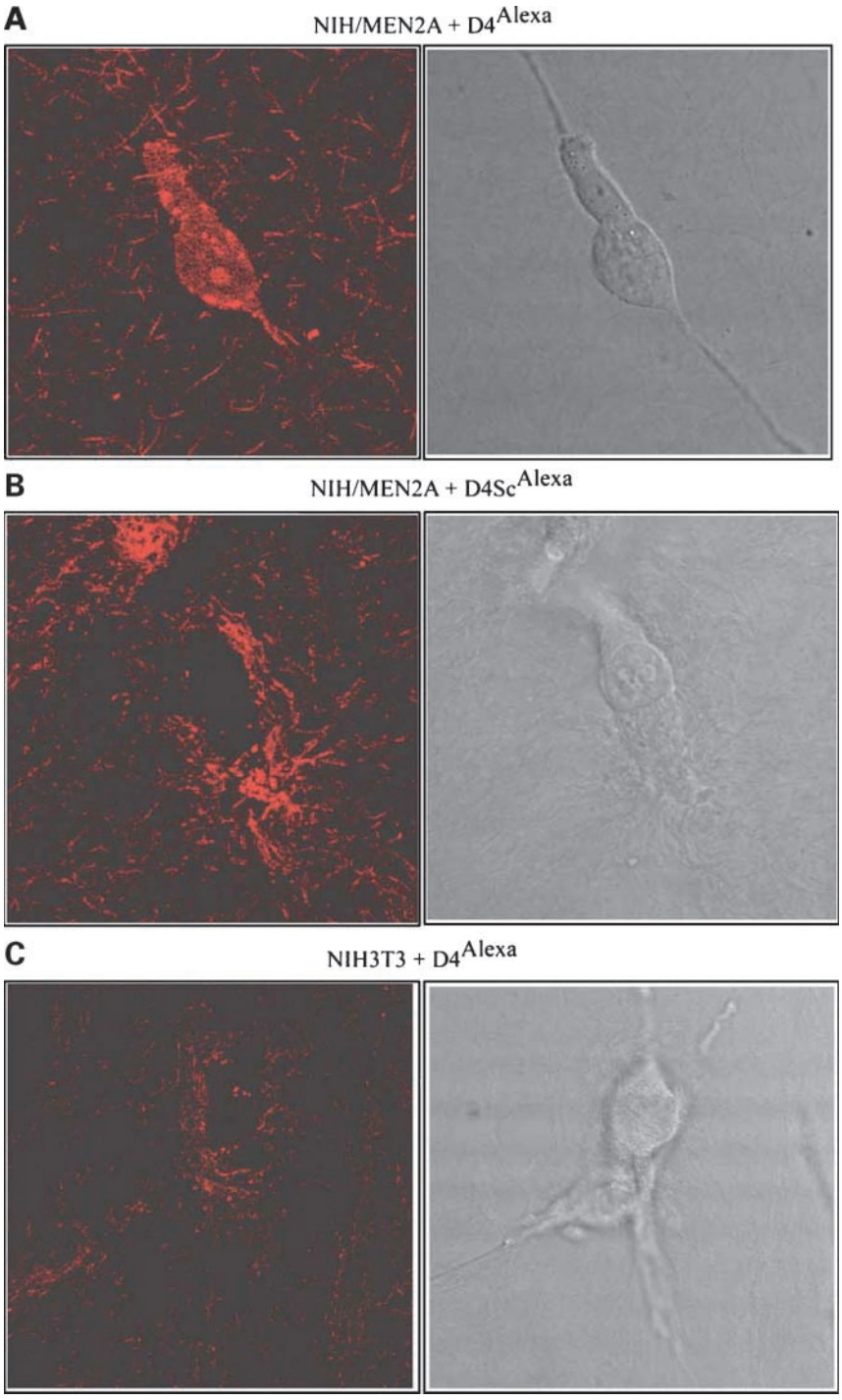

Figure 6. Distribution of D4 aptamer on Ret-expressing cells within three-dimensional gels. **A** and **B,** following treatment with 5 μmol/L $D4^{Alexa}$ and 5 μmol/L $D4Sc^{Alexa}$, respectively, NIH/MEN2A cells embedded in collagen were visualized by confocal microscopy and photographed. **C,** negative control NIH3T3 cells embedded in collagen treated with 5 μmol/L $D4^{Alexa}$.

scanning electron microscopy, the gels consisted of collagen fibrils that form a randomly arranged, entangled network, in agreement with data from literature (11, 12).

As a first attempt, we have determined the collagen concentration and the volume and thickness of the gel matrices, allowing the cells to maintain their physiologic function for long periods in three-dimensional cultures. NIH3T3 and NIH/MEN2A cells encapsulated in type I collagen gels at both 1.2 and 2.4 mg/mL concentrations in complete medium maintain their viability and proliferation for at least 9 days as estimated using direct counting. NIH3T3 cells cultured in three-dimensional matrices at 1.2 mg/mL collagen concentration had the flat and polygonal morphology that characterizes these cells in two-dimensional cultures (data not shown), whereas the NIH/MEN2A cells had a spindle shape, long protrusions,

and high refractive appearance as in two-dimensional cultures (Fig. 5A). The same phenotype was observed in collagen matrix at 2.4 mg/mL concentration (not shown).

Therefore, we asked whether D4 could inhibit Ret^{C634Y} autophosphorylation and receptor-dependent downstream signaling even when the mutated receptor is expressed on the surface of cells encapsulated in collagen matrices. To this aim, D4 or D4Sc was added to NIH/MEN2A cells embedded in collagen, and following 20 h incubation at 37°C, three-dimensional matrices were treated with collagenase and the cell extracts were prepared. As shown by immunoblotting analysis (Fig. 5B, *left*), D4 specifically inhibited the phosphorylation of Ret and its downstream effector ERK with respect to untreated cells (compare *lane 1* with *lanes 2* and *3*). Furthermore, it displays an inhibiting activity strictly comparable with that exhibited on Ret phosphorylation when tested in the two-dimensional NIH/MEN2A cultures (Fig. 5B, *right*). We further insight the consequence of Ret impairment on cell proliferation by monitoring the expression of cell cycle-related protein cyclin D1. As shown, the levels of cyclin D1 were drastically reduced by the D4 treatment of the cells in both two-dimensional and three-dimensional cultures (Fig. 5B).

We then followed the distribution of D4 aptamer on Ret-expressing cells within three-dimensional gels. To this aim, NIH/MEN2A cells embedded in collagen were treated for 20 h at 37°C with $D4^{Alexa}$ (Fig. 6A) or $D4Sc^{Alexa}$ (Fig. 6B) and then visualized by confocal microscopy. As shown, staining the cells with the rhodamine-labeled D4 resulted in a homogeneous distribution of the aptamer on cell surface; conversely, in the presence of the scrambled sequence, a fluorescent staining uniformly distributed in the entire scaffold of the collagen fibers was obtained, whereas no labeled cells were visualized in any of the fields examined. The specificity of the D4 distribution on Ret-expressing cells was confirmed by the absence of fluorescent-aptamer-related signals on NIH3T3 cells within three-dimensional gels following $D4^{Alexa}$ treatment (Fig. 6C).

Nucleic acid aptamers can bind essentially any target protein or molecule based on their specific three-dimensional structures. They have a small size, are poorly (if at all) immunogenic, and can be easily modified; thus, their stability and characteristics for *in vivo* applications can be finely tuned (13–18).

This is the first report of distribution and bioactivity of a nucleic acid-based aptamer in three-dimensional matrices of cells embedded in collagen gel. A great advantage for the use of D4 aptamer in such experimental cell systems is represented by the fact that D4 is a function-blocking compound able to directly interrupt the signal transduction from its target, the Ret receptor. This allows following in three-dimensional cultures not only the aptamer distribution on cell surface but also the outcome of its binding to the target that is the inhibition of Ret activity. Indeed, taken together, our results show that the D4 aptamer fully retains its biological function within three-dimensional cultures. It inhibits the activity of Ret, also when the tyrosine kinase receptor is expressed on the surface of NIH/MEN2A cells that have been suspended throughout collagen gels. The specificity combined to the low molecular weight and the high stability of D4 prompt us to investigate the behavior of the aptamer in physiologically relevant *in vivo*-like, cell-derived three-dimensional matrices. In conclusion, the ability of D4 aptamer to retain the conformation that allows to hit and inhibit its target in three-dimensional collagen matrices provides a strong experimental base to its use *in vivo* in animal models of tumors.

Disclosure of Potential Conflicts of Interest

No potential conflicts of interest were disclosed.

Acknowledgments

We thank Drs. Domenico Libri and Ingram Iaccarino Idelson for helpful discussion, Salvatore Arbucci for assistance with confocal microscopy, and Giuseppina Ippolito for editing assistance.

References

1. Meng X, Lindahl M, Hyvönen ME, et al. Regulation of cell fate decision of undifferentiated spermatogonia by GDNF. Science 2000; 287:1489 – 93.

2. Sariola H, Saarma M. Novel functions and signalling pathways for GDNF. J Cell Sci 2003;116:3855 – 62.

3. Cerchia L, Ducongé F, Pestourie C, et al. Neutralizing aptamers from whole-cell SELEX inhibit the RET receptor tyrosine kinase. PLoS Biol 2005; 3:123.

4. Pestourie C, Cerchia L, Gombert K, et al. Comparison of different strategies to select aptamers against a transmembrane protein target. Oligonucleotides 2006;16:323 – 35.

5. Esposito CL, D'Alessio A, De Franciscis V, Cerchia L. A cross-talk between TrkB and Ret tyrosine kinases receptors mediates neuroblastoma cells differentiation. PLoS ONE 2008;3:1643.

6. Saltzman WM, Parkhurst MR, Parsons-Wingerter P, Zhu WH. Three-dimensional cell cultures mimic tissues. Ann N Y Acad Sci 1992;665:259 – 73.

7. Campbell RB. Tumor physiology and delivery of nanopharmaceuticals. Anticancer Agents Med Chem 2006;6:503 – 12.

8. Griffith LG, Swartz MA. Capturing complex 3D tissue physiology *in vitro*. Nat Rev Mol Cell Biol 2006;7:211 – 24.

9. Cerchia L, Libri D, Carlomagno MS, de Franciscis V. The soluble ectodomain of RetC634Y inhibits both the wild-type and the constitutively active Ret. Biochem J 2003;372:897 – 903.

10. Haustein E, Schwille P. Fluorescence correlation spectroscopy: novel variations of an established technique. Annu Rev Biophys Biomol Struct 2007;36:151 – 69.

11. Ramanujan S, Pluen A, McKee TD, Brown EB, Boucher Y, Jain RK. Diffusion and convection in collagen gels: implications for transport in the tumor interstitium. Biophys J 2002;8:1650 – 60.

12. Mahoney MJ, Krewson C, Miller J, Saltzman WM. Impact of cell type and density on nerve growth factor distribution and bioactivity in 3-dimensional collagen gel cultures. Tissue Eng 2006;12:1915 – 27.

13. Tuerk C, Gold L. Systematic evolution of ligands by exponential enrichment: RNA ligands to bacteriophage T4 DNA polymerase. Science 1990;249:505 – 10.

14. Nimjee SM, Rusconi CP, Sullenger BA. Aptamers: an emerging class of therapeutics. Annu Rev Med 2005;56:555 – 83.

15. Eyetech Study Group. Preclinical and phase IA clinical evaluation of an anti-VEGF pegylated aptamer (EYE001) for the treatment of exudative age-related macular degeneration. Retina 2002;22:143 – 52.

16. Hicke BJ, Stephens AW. Escort aptamers: a delivery service for diagnosis and therapy. J Clin Invest 2000;106:923 – 8.

17. Cerchia L, Hamm J, Libri D, et al. Nucleic acid aptamers in cancer medicine. FEBS Lett 2002;528:12 – 6.

18. Cerchia L, de Franciscis V. Nucleic acid-based aptamers as promising therapeutics in neoplastic diseases. Methods Mol Biol 2007; 361:187 – 200.

Molecular Cancer Therapeutics

Distribution and bioactivity of the Ret-specific D4 aptamer in three-dimensional collagen gel cultures

Maria Teresa Vento, Marco Iuorio, Paolo A. Netti, et al.

Mol Cancer Ther 2008;7:3381-3388.